Neurosci. Bull. June, 2024, 40(6):695–706
https://doi.org/10.1007/s12264-023-01132-8

www.neurosci.cn
www.springer.com/12264

ORIGINAL ARTICLE

Mechanism of Endogenous Peptide PDYBX1 and Precursor Protein YBX1 in Hirschsprung's Disease

Qiaochu Sun[1] · Zhengke Zhi[1] · Chenglong Wang[1] · Chunxia Du[1] · Jie Tang[1] · Hongxing Li[1] · Weibing Tang[1]

Received: 6 March 2023 / Accepted: 12 August 2023 / Published online: 1 October 2023

Abstract Endogenous peptides, bioactive agents with a small molecular weight and outstanding absorbability, regulate various cellular processes and diseases. However, their role in the occurrence of Hirschsprung's disease (HSCR) remains unclear. Here, we found that the expression of an endogenous peptide derived from YBX1 (termed PDYBX1 in this study) was upregulated in the aganglionic colonic tissue of HSCR patients, whereas its precursor protein YBX1 was downregulated. As shown by Transwell and cytoskeleton staining assays, silencing YBX1 inhibited the migration of enteric neural cells, and this effect was partially reversed after treatment with PDYBX1. Moreover, immunoprecipitation and immunofluorescence revealed that ERK2 bound to YBX1 and PDYBX1. Downregulation of YBX1 blocked the ERK1/2 pathway, but upregulation of PDYBX1 counteracted this effect by binding to ERK2, thereby promoting cell migration and proliferation. Taken together, the endogenous peptide PDYBX1 may partially alleviate the inhibition of the ERK1/2 pathway caused by the downregulation of its precursor protein YBX1 to antagonize the impairment of enteric neural cells. PDYBX1 may be exploited to design a novel potential therapeutic agent for HSCR.

Qiaochu Sun and Zhengke Zhi contributed equally to this work.

Supplementary Information The online version contains supplementary material available at https://doi.org/10.1007/s12264-023-01132-8.

✉ Hongxing Li
hx8817@njmu.edu.cn

✉ Weibing Tang
twbcn@njmu.edu.cn

[1] Department of Pediatric Surgery, Children's Hospital of Nanjing Medical University, Nanjing 210008, China

Keywords Hirschsprung's disease · YBX1 · Endogenous peptide · PDYBX1 · Enteric neural cell

Introduction

Hirschsprung's disease (HSCR), a serious congenital defect, occurs as the colonization of enteric neural crest cells (ENCCs) fails [1]. With a global prevalence of ~ 1/2000–1/5000 [2], HSCR is mainly manifested by difficult defecation and functional intestinal obstruction [3–5]. Surgery is the primary treatment for HSCR but is followed by long-term complications, such as recurrent constipation, fecal incontinence, and enterocolitis [6, 7]. RET, EDNRB, SOX10, and PHOX2B have been confirmed to be closely implicated in the occurrence of HSCR [8]; however, its pathogenic mechanism remains to be fully elucidated.

Studies in peptidomics have shown that endogenous peptides play critical roles in physiological activities, just as macromolecular proteins do. A class of small-molecular-weight peptides produced *in vivo*, endogenous peptides are involved in multiple biological processes, including metabolic regulation, signal transduction, and the maintenance of cell functions [9]. Notably, endogenous peptides are involved in the regulation of the activities of the nervous system. NAPVSIPQ and SALLRSIPA, derived from an activity-dependent neuroprotective protein (ADNP) and activity-dependent neurotrophic factor (ADNF), safeguard the stability of microtubules and transport in axons [10]. In addition, The VGF peptide derived from the carboxyl-terminal of a neurosecretory protein is associated with spinal neuroplasticity. Upon nerve injury, its level is upregulated, and this can be considered a signal of peripheral nerve injury [11]. Moreover, the endogenous peptide FGL, produced by nerve cell adhesion molecules, boosts synaptogenesis and

the proliferation of stem cells, thus facilitating recovery from stroke [12]. Nevertheless, few studies have been carried out to verify the role of endogenous peptides during the development of the enteric nervous system (ENS).

Here, we found a new stable endogenous peptide derived from YBX1 that was upregulated in the aganglionic tissue of HSCR patients. To date, it has appeared in none of the previous studies, thus we named it PDYBX1 (peptide derived from YBX1) for further research. Precursor proteins undergo shearing and modification, eventually converting into multiple endogenous peptides that perform various physiological functions, as their precursor proteins do [13, 14]. Interestingly, we found that YBX1, the precursor protein of PDYBX1, was markedly downregulated in the aganglionic segment of HSCR tissue and suppressed the migration of enteric neural cells. As is well known, the YBX1 protein belongs to the cold shock protein family, which binds to target genes through the highly conserved cold shock domain, affects the transcription and translation of downstream genes, and is closely related to cell migration and proliferation [15]. YBX1 is one of the proteins associated with a large number of human diseases that have been studied and is of great importance in early embryonic development, differentiation, and stress [16]. In addition, YBX1 plays an important role in regulating signaling pathways and maintaining cell functions [17, 18]. In cancer research, it has been found that YBX1 expression is associated with the tumorigenic transformation of cells, and increased YBX1 expression promotes the progression of colorectal cancer, gastric cancer, central nervous system tumors, and other diseases [19–22]. However, the role of YBX1 in the occurrence of HSCR has not been reported.

In the present study, we aimed to clarify the function of PDYBX1 and YBX1 in the migration of enteric neural cells, as well as their relationship, in which PDYBX1 might partly antagonize the impairment of enteric neural cell migration caused by downregulation of its precursor protein YBX1, thus providing a new target for the treatment of HSCR.

Materials and Methods

Clinical Samples

Dilated and aganglionic colon tissue was collected from 24 HSCR patients, and control colon tissue was harvested from patients without enteric nervous malformation at the Children's Hospital of Nanjing Medical University and immediately stored at − 80 °C. All HSCR patients were diagnosed through pathological analysis. This study was approved by the Institutional Ethics Committee of the Children's Hospital of Nanjing Medical University (approval number: 202210180-1).

Cell Culture

SK-N-BE2 cells were from Procell (Wuhan, China), and cultured with DMEM/F12 (Gibco, C11330500BT) containing 10% fetal bovine serum (Procell, 164210-500) and 1% penicillin-streptomycin-amphotericin B solution (Procell, PB180121). Enteric neural precursor cells (ENPCs) were isolated from C57BL/6J mice for 16.5 gestational days provided by the Animal Core Facility of Nanjing Medical University. The neural marker proteins Calretinin and Nestin were detected in ENPCs (Fig. S1A). Briefly, fetal mice were isolated from anesthetized pregnant mice. The intestinal tracts of fetal mice were separated, and the mesentery was carefully removed under an anatomical microscope. Subsequently, the intestinal tissue was cut into 1 mm^3 pieces and incubated in collagenase IV (1 mg/mL, Sigma, C5138-25MG) at 37 °C for 30 min. After filtration with 70 μm and 37 μm cell meshes, the filtrates were collected and centrifuged at 1000 rpm for 5 min at room temperature. The precipitate was resuspended and cultured with a complete culture medium of mouse intestinal neural crest stem cells (Procell, CM-M216). All cells were cultured in an incubator with suitable humidity and 5% CO_2 at 37 °C.

Cell Transfection

Small interfering RNAs (siRNAs) were designed by Genepharma (Shanghai, China), and overexpression plasmids were obtained from Genechem (Shanghai, China). Lipofectamine 3000 (ThermoFisher, USA) was used for cell transfection according to the manufacturer's instructions. The sequences of siRNAs and plasmids are listed in Table S1.

Real-time Quantitative Polymerase Chain Reaction (RT-PCR)

TRIzol reagent (Life Technologies, USA) was used to isolate RNA from tissues and cells, and a NanoDrop 2000 spectrophotometer was applied to assess the concentration and purity of extracted RNA. RNA was reverse-transcribed into cDNA using a reverse transcription kit (R323-01-AC Vazyme, China), followed by RT-qPCR using ChamQ SYBR qPCR Master Mix (Q311-02-AA Vazyme, China). The processes of degeneration, annealing, and extension were repeated for 40 circulations. The relative gene expression level was calculated using the $2^{-\Delta\Delta CT}$ method [23]. GAPDH was applied as the internal reference. The primers used in this study are listed in Table S1.

Western Blot

RIPA buffer (Beyotime, China) was applied to extract proteins from tissues and cells. The protein concentration was

determined by the bicinchoninic acid method (Beyotime, China). The proteins (60 μg per lane) were separated on 10% SDS-PAGE gel and then transferred to a polyvinylidene fluoride membrane (Merck, USA). Afterward, the membranes were blocked with 5% fat-free milk at room temperature for 2 h. Having been washed three times with TBST, the membranes were incubated with primary antibodies (anti-YBX1 1:2000, 20339-1-AP, Proteintech, China; anti-ERK2 1:2000, ab32081, Abcam, USA; anti-ERK1 1:1000 ab32537, Abcam, USA; anti-6xHistag 1:1000, ab18184, Abcam, USA; phospho-p44/42 MAPK (p-ERK1/2) 1:1500, #4370, CST, USA; anti-GAPDH 1:1500, ab8245, Abcam, USA) at 4 °C overnight. The corresponding secondary antibodies (HRP-labeled goat anti-rabbit IgG(H + L) 1:1000, A0208, Beyotime, China; HRP-labeled goat anti-mouse IgG(H + L) 1:1000, A0216, Beyotime, China) were then used for another 2 h incubation at room temperature. Finally, the membranes were exposed with an ECL chemiluminescence kit (P10050, NcmBiotech Ultra, China) under an exposure meter (Tanon, Shanghai). The gray value was calculated using ImageJ software (National Institutes of Health, USA).

Ethynyl Deoxy Uridine (EdU)

Cells were inoculated onto 96-well plates at a density of 1×10^4 cells per well, and cultured for 24 h–48 h. After that, an EdU medium was applied to treat cells. Then, cells were fixed with 4% paraformaldehyde for 20 min. The EdU assay was performed according to the manufacturer's protocol with the EdU kit (Ribobio, China). The positive EdU staining cells were detected using Cellnsight (ThermoFisher, USA) at 20 magnifications.

Cell Migration

Cell migration was measured using a Transwell assay. A total of 2×10^4 cells resuspended in the serum-free medium were planted into the upper chamber, and 600 μL of complete medium was added into the bottom chamber. After incubation for 24 h–48 h, the migrated cells were fixed with 4% paraformaldehyde for 30 min and then stained with crystal violet (Beyotime, China). Cell images were captured on an inverted microscope (×20, Nikon, Japan).

Cytoskeleton Staining

Around 2×10^4 cells were seeded into laser confocal dishes, cultured for 24 h–48 h, fixed in 4% paraformaldehyde, treated with 0.5%Triton X-100, incubated with 200 μl TRITC Phalloidin (Yeasen, China) working solution at room temperature in the dark for 30 min, and finally stained with DAPI (0100-20, SouthernBiotech). The cytoskeletal morphology was observed under an LSM700 laser confocal microscope (Zeiss, Germany). The fluorescence intensity was quantified using ImageJ (National Institutes of Health, USA).

Synthesis of Peptides

Peptides, including PDYBX1 (NPPVQGEVMEGADNQGAGEQGRPVR), His-PDYBX1 (peptide with Histag), and FITC-PDYBX1 (peptide with FITC tag), were synthesized by BNQ Biotech (Nanjing) Ltd.

Enzyme-Linked Immunosorbent Asay (ELISA)

The ELISA kit for endogenous peptides was provided by BNQ Biotech (Nanjing). Briefly, total endogenous peptides were isolated from tissues and added to a solid-phase polystyrene enzyme plate (100 μL/well) to be incubated for 12 h at 4 °C. Afterward, the unbound peptides were washed three times with a washing buffer. The blocking buffer was used to block the non-specific binding at room temperature for 2 h. The specific antibody for PDYBX1 (BNQ Biotech, Nanjing) was added to each well and incubated at room temperature for 1 h. After three washes, the samples were incubated with goat anti-rabbit IgG labeled with HRP for 30 min at 37 °C. Then, 100 μL of substrate was added to each well for 1.5-h incubation at room temperature in the dark. Finally, the absorbances of each sample at 450 nm and 620 nm were recorded with a microplate reader.

Immunoprecipitation (IP)

IP was applied using an IP kit (88804, ThermoFisher, USA). Cells were washed with PBS and subsequently incubated with pre-cooled IP lysis solution for 5 min on ice. The supernatant was collected after centrifugation (12,000*g*, 10 min, 4 °C). Appropriate YBX1 and Histag primary antibodies were added to the supernatant for incubation at 4 °C overnight to form immune complexes. The antigen/antibody mixture was then added to a centrifuge tube containing prewashed magnetic beads and incubated at room temperature for 1 h. Subsequently, 500 μL of IP washing buffer was added to wash the magnetic beads three times, and 100 μL of elution buffer was then added to the centrifuge tube for incubation at room temperature for 10 min–15 min. The magnetic beads were separated, and the supernatant containing the immune complex was preserved. Finally, Western blot was used to detect the expression of ERK2.

Immunofluorescence

For immunofluorescence, cells were fixed with 4% paraformaldehyde for 30 min and then treated with 0.5% Triton X-100 for 20 min and 3% H_2O_2 for 5 min. The immunofluorescence

blocking reagent (Beyotime, P0220, China) was applied to block cells for 20 min. Subsequently, appropriate primary antibodies were added for incubation overnight at 4 °C. The corresponding secondary antibodies were used to incubate cells at 37 °C for another 30 min. Finally, DAPI Fluoromount-G (SouthernBiotech, 0100-20, USA) was added. To verify the colocalization of YBX1 and ERK2, TSA (Tyramide signal amplification), which can mark proteins challenged with any type of antibodies, was applied based on the product manual. Finally, the fluorescence was observed under a laser confocal microscope (×63, LSM700, Zeiss, Germany) to reflect the colocalization of PDYBX1 (or YBX1) and ERK2 in cells.

Zebrafish Model

The morpholino (MO) target YBX1 (MO-YBX1) was designed by GeneTools (USA). The zygotes of zebrafish at the single-cell stage were collected and injected with MO-YBX1 (4 ng) and PDYBX1 (6 μmol/L). The zebrafish were collected at 120 h post-fertilization (hpf). For the immunofluorescence assay, the zebrafish were washed 3 times with 1% Triton X-100 for 5 min, followed by quick washing with pre-cooled ddH_2O for 5 min. Icy acetone was used for permeabilization for 10 min. Next, the zebrafish were washed with 1% Triton X-100 for 5 min, blocked with 10% sheep serum + 1% DMSO at room temperature for 1.5 h, and then incubated with anti-HuC/D (A-21271, Thermofisher, USA) at 4 °C for 1 week. Finally, the zebrafish were incubated with the corresponding fluorescent secondary antibodies overnight at room temperature and photographed under a stereo-fluorescence microscope (×5, LSM700, Zeiss, Germany).

Animals

Ednrb$^{-/-}$ C57BL/6J mice were generated by Biocytogen Co. (Beijing, China) using CRISPR/Cas9-based non-homologous end joining and maintained in the Animal Center of Nanjing Medical University. After mating with heterozygotes, the Ednrb$^{+/-}$ pregnant mice were treated with PDYBX1 (1 mg/kg) through the tail vein every day from E9.5 to E14.5 days of pregnancy. Meanwhile, the pregnant mice injected with the same volume of ddH_2O were assigned to the control group. All the animal experiments were performed according to the guidelines and protocols and approved by the Animal Care & Welfare Committee of Nanjing Medical University (approval number: IACUC2107040).

In vivo Imaging

In vivo, fluorescence imaging was carried out using IVIS Spectrum (PerkinElmer, USA). Briefly, the pregnant C57BL/6J mice at E14.5 were injected with FITC-labeled PDYBX1 (FITC-PDYBX1, 1 mg/kg) *via* the tail vein referring to a previous study [24]. After 12 h, the mice were anesthetized, and the *in vivo* fluorescence imaging was performed. Afterward, the embryos were harvested and subjected to *in vitro* fluorescence imaging.

Whole-Mount Immunofluorescence Staining

Intestinal tissue samples were collected from each group of mouse embryos at E16.5 and subsequently fixed with 4% PFA solution for 12 h. Then, the tissues were washed with PBS for 30 min, which was repeated three times. Dent's Fix solution (methanol:DMSO = 4:1) was used for another 12 h fixation. After washing three times, the intestines were incubated with anti-Tuj1 (1:200, ab18207, Abcam, USA) for 3 days at 4 °C. After that, the corresponding Alexa Fluor 488 AffiniPure secondary antibody (33906ES60, Yeasen, China) was added and incubated for 2 days at 4 °C. Finally, the confocal laser microscope (LSM900, Zeiss, Germany) was applied to observe the intestinal tissue.

Statistical Analysis

GraphPad Prism 8 (GraphPad Software, USA) was used for statistical analysis. Data are presented as the mean ± SD. Unpaired Student's t-test was used to analyze differences between the two groups, while the one-way ANOVA was followed by Turkey's to analyze differences among multiple groups. A difference was considered statistically significant when $P < 0.05$.

Results

PDYBX1 is Upregulated in Aganglionic Colon Tissue from HSCR Patients

In the peptidomics analysis conducted in our previous study [25], the endogenous peptide PDYBX1 derived from the YBX1 protein attracted our attention. Its amino-acid sequence was "NPPVQGEVMEGADNQGAGEQGRPVR". The analysis based on the ProtParam database showed its molecular weight to be 2592.78Da, the isoelectric point was 4.41, the half-life *in vivo* was > 10 h, the instability coefficient was 27.73, the grand average hydropathicity was − 1.168, and the fat solubility index was 42.80 (Fig. S1B). These parameters indicate that PDYBX1 has high stability, strong liposolubility, and a long half-life *in vivo*. Notably, we found that PDYBX1 was upregulated in the aganglionic colon tissue from HSCR patients by ELISA (Fig. 1A), whereas its precursor protein YBX1 was downregulated at the mRNA and protein levels (Fig. 1B, C). The above

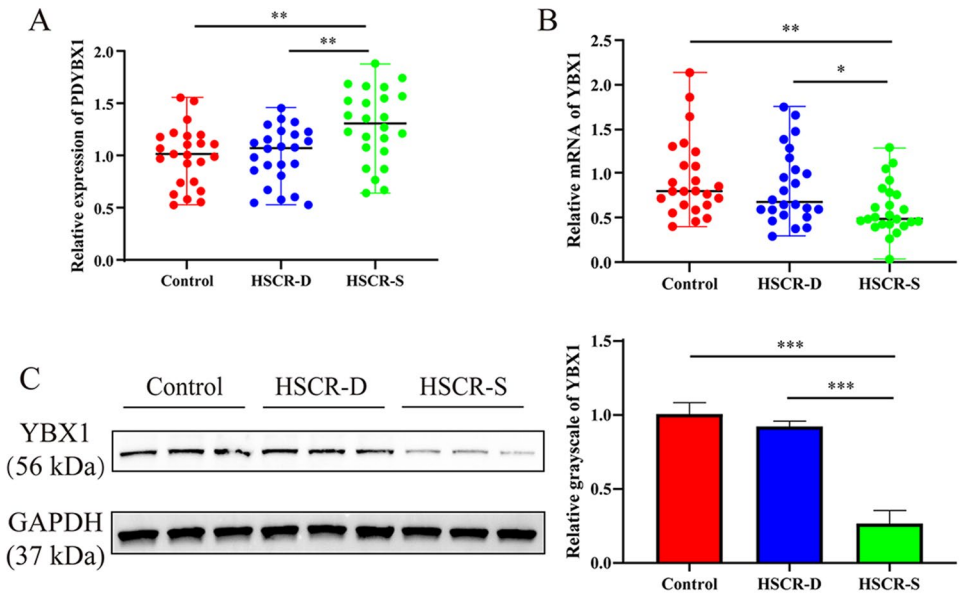

Fig. 1 PDYBX1 is upregulated in aganglionic colon tissue from HSCR patients. **A** The expression of PDYBX1 in HSCR aganglionic colon tissue, dilated colon tissue, and control colon tissue as detected by ELISA. Each group contains 24 samples. **B** qRT-PCR analysis of YBX1 expression in HSCR aganglionic, dilated, and control colon tissues ($n=24$). **C** Western blots and analysis of YBX1 expression in HSCR and control samples ($n=3$). HSCR-D: dilated colon segment of HSCR patient, HSCR-S: stenotic colon segment of HSCR patient $^{*}P<0.05$; $^{**}P<0.01$; $^{***}P<0.001$.

findings inspired us to further explore the role of overexpressed PDYBX1 and down-regulated YBX1, as well as their interaction during the occurrence of HSCR.

Silencing YBX1 Inhibits the Migration of Enteric Neural Cells

YBX1, a member of a cold shock protein family, can pass through the highly conserved cold shock domain and bind to the target gene to promote cell migration and proliferation [15, 17, 26, 27]. Transwell assays showed that cellular migration was markedly inhibited when the expression of YBX1 was silenced using siYBX1 (Fig. S1C, D) in SK-N-BE2 cells and ENPCs (Fig. 2A). Besides, the fluorescence intensity of the cytoskeleton was markedly reduced when YBX1 was knocked down in both SK-N-BE2 cells and ENPCs (Fig. 2B). In addition, EdU assays showed that fewer cells proliferated in the YBX1 knockdown group than in the control group (Fig. 2C, D). The above results indicated that downregulation of YBX1 might repress the migration of enteric neural cells, as well as their proliferation.

PDYBX1 Promotes the Migration of Enteric Neural Cells

It is well known that endogenous peptides share some functions similar to their precursor proteins. To clarify the effect of PDYBX1 on the migration of enteric neural cells, ENPCs, and SK-N-BE2 cells were incubated with synthetic PDYBX1. Firstly, immunofluorescence showed that FITC-PDYBX1 was absorbed by SK-N-BE2 cells and ENPCs (Fig. 3A). Furthermore, Transwell and cytoskeletal staining assays showed that the migration of SK-N-BE2 cells and ENPCs was markedly enhanced by PDYBX1 at a dose of 20 μg/mL (Fig. 3B, C). Meanwhile, EdU assays confirmed that PDYBX1 promoted the proliferation of SK-N-BE2 cells and ENPCs (Fig. 3D).

PDYBX1 Upregulation Reverses the Migration-Inhibiting Effect of YBX1 Downregulation on Enteric Neural Cells

We further explored whether PDYBX1 upregulation could partly antagonize the inhibitory effects induced by YBX1 silencing. According to the results of Transwell and cytoskeletal staining assays, when SK-N-BE2 cells and ENPCs were simultaneously treated with PDYBX1, the cellular migration was markedly enhanced, compared to that in the YBX1 knockdown group (Fig. 4A, B). Moreover, the EdU assays revealed that the proliferation of SK-N-BE2 cells and ENPCs, which had been inhibited by YBX1 knockdown, could be partly reversed by PDYBX1 (Fig. 4C).

YBX1 Functions by Activating the ERK1/2 Pathway

YBX1 can bind to ERK2 specifically to influence the ERK1/2 pathway [28]. Here, we tested whether YBX1 regulates the proliferation of enteric neural cells by binding to ERK2. As the IP assay showed, ERK2 protein was enriched by anti-YBX1, but not anti-IgG (Fig. 5A). TSA showed the colocalization of YBX1 and ERK2 under the laser confocal microscope (Fig. 5B), confirming the interaction between the YBX1 and ERK2 proteins. Moreover, when YBX1 was knocked down in SK-N-BE2 cells, the protein levels of ERK2 and p-ERK1/2 were markedly decreased, but ERK1 expression did not change significantly (Fig. 5C). Notably,

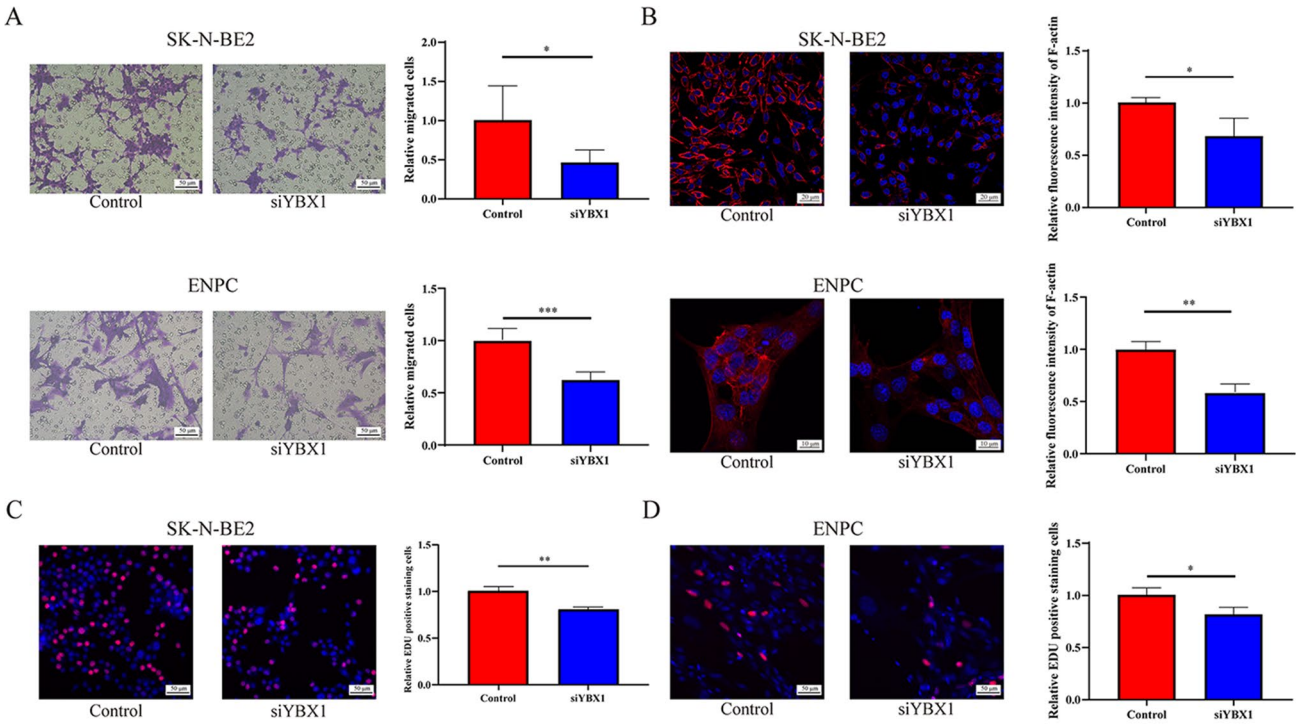

Fig. 2 Silencing of YBX1 inhibits the migration of enteric neural cells. **A** YBX1 down-regulation attenuates the migration of SK-N-BE2 cells and ENPCs (×20 magnification). **B** Silencing of YBX1 breaks the formation of the cytoskeleton compared with controls in SK-N-BE2 cells and ENPCs. Blue indicates the nucleus and red indicates the F-actin of the cytoskeleton (×63 magnification). **C**, **D** EdU assays show the impairment of cell proliferation caused by downregulating YBX1 (×20 magnification). All cell function experiments were set up in triplicate ($n=3$). *$P<0.05$; **$P<0.01$; ***$P<0.001$.

the inhibitory effect of YBX1 downregulation on cellular migration was reversed by the overexpression of ERK2 in SK-N-BE2 cells and ENPCs (Fig. 5D, E). Furthermore, the introduction of ERK2 restored cellular proliferation that had been attenuated by the knockdown of YBX1 (Fig. 5F). These results illustrated that YBX1 can activate the ERK1/2 signaling pathway by directly binding to ERK2 protein, and YBX1 downregulation might repress cellular migration by blocking the ERK1/2 pathway.

PDYBX1 Activates the ERK1/2 Pathway to Promote the Migration of Enteric Neural Cells

By using SMART (simple modular architecture research tool) analysis, we found that the sequence of PDYBX1 was located in the carboxyl-terminal of YBX1 (see diagram in Fig. 6A). The ending of the carboxyl-terminal (aa 130-324) of YBX1 is responsible for its interaction with other proteins [29]. Therefore, we proposed that PDYBX1 might bind to ERK2 to activate the ERK1/2 pathway, thereby reversing the inhibitory effects caused by the downregulation of YBX1. The Histag protein-labeled His-PDYBX1 was used to conduct IP and immunofluorescence assays in SK-N-BE2 cells, and the results verified that PDYBX1 was able to bind to ERK2 (Fig. 6B, C). Besides, in SK-N-BE2 cells treated with PDYBX1, the expression of ERK2 and p-ERK1/2 was markedly raised, whereas that of ERK1 showed no significant change (Fig. 6D). Furthermore, knockdown of YBX1 decreased the expression of ERK2 and p-ERK1/2, but PDYBX1 partly reversed this decrease (Fig. 6E). In SK-N-BE2 cells and ENPCs, ERK2 silencing impaired the migratory capacity of cells, but PDYBX1 reversed this impairment (Fig. 6F, G). The cellular proliferation showed a similar tendency, as indicated by EdU assays (Fig. 6H). Taken together, PDYBX1 might antagonize the inhibition of cellular migration induced by YBX1 downregulation *via* activating the ERK1/2 signaling pathway.

PDYBX1 Protects the Formation of the ENS *in vivo*

To further investigate the role of YBX1 and PDYBX1 in the development of the ENS, the zebrafish model was applied and the anti-HuC/D antibody was used to assess the development of enteric neurons. The zebrafish were randomly divided into four groups treated at zygophase with PBS, MO-YBX1, PDYBX1, or MO-YBX1+PDYBX1. Finally, all zebrafish were collected at 120 hpf. The HuC/D$^+$ cells were fewer in the YBX1 knockdown (using MO-YBX1)

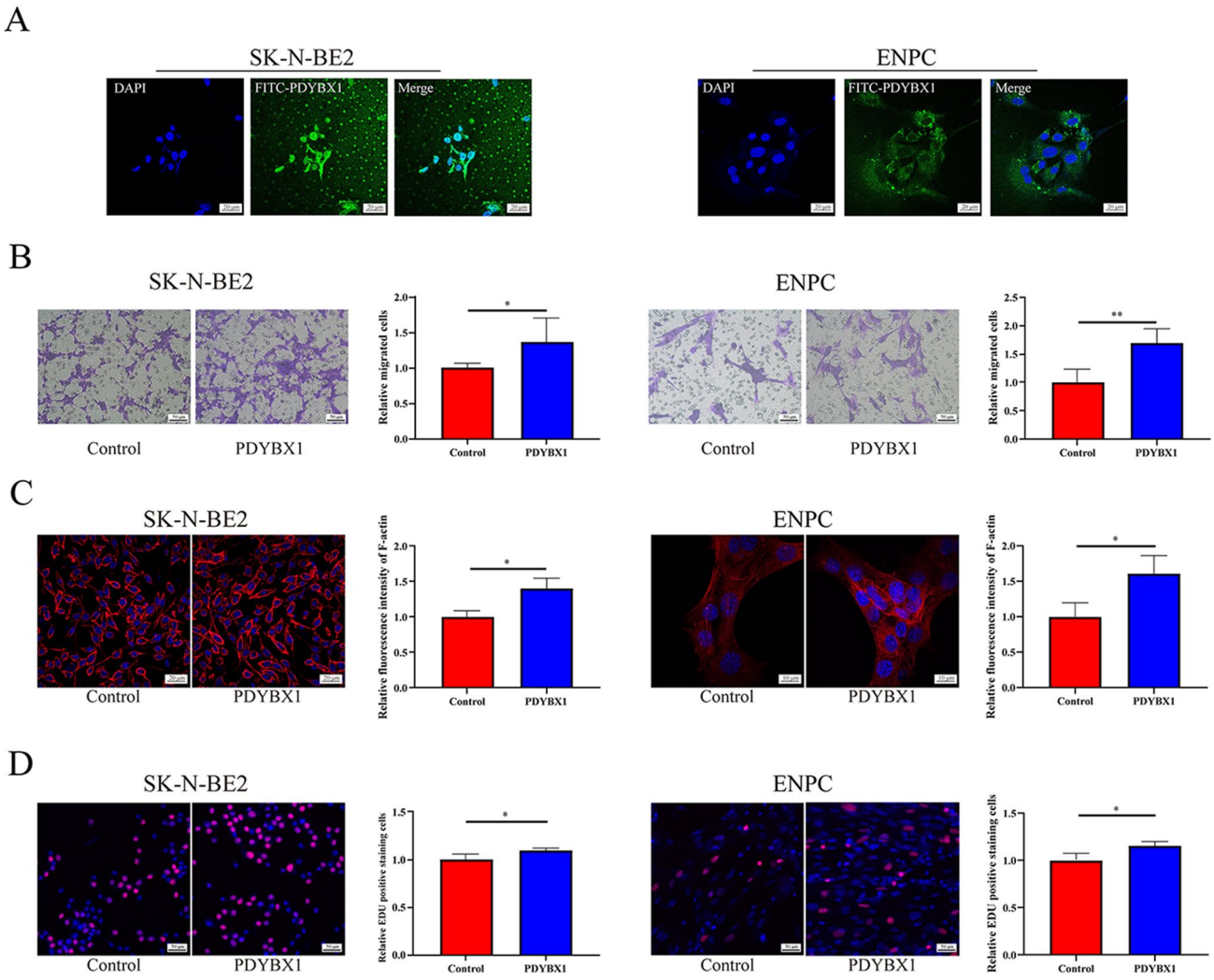

Fig. 3 Overexpressed PDYBX1 promotes the migration of neural cells. **A** Immunofluorescence showing that FITC-PDYBX1 can be taken up by SK-N-BE2 cells and ENPCs. Blue indicates the nucleus and green comes from FITC-PDYBX1 (×63 magnification). **B** Treatment with PDYBX1 increases the migration rate of SK-N-BE2 cells and ENPCs (×20). **C** Silencing YBX1 inhibits the formation of the cytoskeleton compared with controls in SK-N-BE2 cells and ENPCs (×63). **D** In SK-N-BE2 cells and ENPCs, EdU assays show that supplementation with PDYBX1 increases the number of positive EdU stained cells (×20). All cell function experiments were carried out in triplicate. $*P<0.05$; $**P<0.01$.

group than in the control group and failed to migrate to the end of the intestine (Fig. 7A). However, HuC/D$^+$ cells flourished after injection of PDYBX1 (Fig. 7B). Notably, we found that simultaneous treatment with PDYBX1 also induced more cells to migrate to the terminal of intestine compared to those in the MO-YBX1 group, indicating the protective role of PDYBX1 in the formation of the ENS (Fig. 7C). In addition, the Ednrb$^{-/-}$ mouse model, which is a commonly used animal model of HSCR, was used to further validate the therapeutic potential of PDYBX1 *in vivo*. To determine whether PDYBX1 can cross the placental barrier and reach the embryos, pregnant mice at E14.5 were treated with FITC-PDYBX1 (1 mg/kg). After 12 h, the fluorescence signal could be observed in the mouse, indicating the absorption of PDYBX1. Moreover, the fluorescence was also present in the embryos, showing that PDYBX1 had reached them (Fig. S1E). Within the E9.5-14.5 window of ENS development, pregnant Ednrb$^{+/-}$ mice were treated with PDYBX1, while mice treated with ddH_2O served as the control group. At E16.5, the intestines of all the embryos in each group were harvested, and the intestinal tissues from Ednrb$^{-/-}$ embryos were selected for further whole-mount staining using anti-Tuj1. As shown in Fig. 7D, PDYBX1 treatment improved the formation of the ENS in the HSCR mouse by promoting the migration of enteric neural cells, compared to the HSCR mice treated with ddH_2O. Therefore, PDYBX1 can partly promote the formation of the ENS by enhancing the migration of enteric neural cells, providing

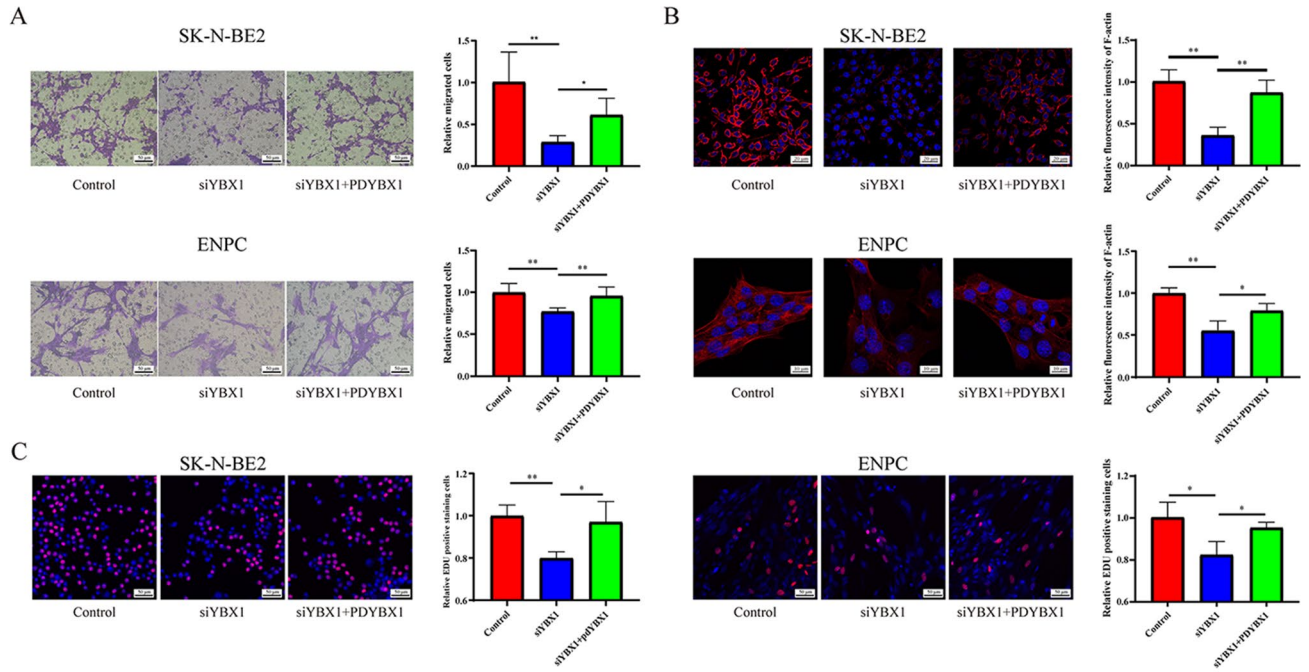

Fig. 4 PDYBX1 reverses the inhibitory effect on cell migration caused by silencing YBX1. **A**, **B** Supplementation with PDYBX1 reverses the impaired migration (×20 magnification) and cytoskeletal deficit (×63) of SK-N-BE2 cells and ENPCs caused by the knockdown of YBX1. **C** EdU assays indicate that PDYBX1 can reverse the cell proliferation which was inhibited by the silencing of YBX1 (×20). All cell function experiments were carried out in triplicate. $^{*}P < 0.05$; $^{**}P < 0.01$.

a novel therapeutic strategy for HSCR by supplementing PDYBX1.

Discussion

Mounting evidence suggests that, as the intestinal microenvironment is disrupted during embryonic development, genetic factors may contribute to the abnormal migration of enteric neural crest cells, or ultimately HSCR [30]. Although plentiful studies have explored susceptibility genes and the related cellular and molecular mechanisms, the etiology of HSCR has not been fully explained. Peptidomics has provided a novel direction in the exploration of the etiopathogenesis of HSCR. Our previous peptidomic study has revealed that a peptide derived from AHNAK (termed PDAHNAK) might cooperate with its precursor protein AHNAK to inhibit the migration of ENCCs in HSCR [25]. However, whether other abnormal endogenous peptides are involved in HSCR, and their mechanisms in HSCR remain to be unveiled. In the present study, we found that the endogenous peptide PDYBX1 was up-regulated in the aganglionic segment of HSCR, and treatment with PDYBX1 significantly promoted the migration of enteric neural cells, indicating the potential therapeutic effect of PDYBX1 on HSCR. Besides, we found that PDYBX1 was higher in the stenotic segment than in the dilated segment, while its precursor protein YBX1 showed no significant difference. This might be owing to the compensatory enrichment of PDYBX1 in the diseased segment during the progression of HSCR.

PDYBX1 is derived from YBX1, and YBX1 is dysregulated in several human diseases [31, 32]; however, the role of YBX1 in HSCR is still not clear. In the present study, we found that the expression of YBX1 was suppressed in HSCR. By *in vitro* and *in vivo* experiments, we clarified that this suppression was associated with hindered ENS growth and might drive the occurrence of HSCR. Based on the above results, we wondered whether the upregulated PDYBX1 could antagonize the inhibitory effects caused by the downregulated YBX1. Furthermore, the migration of SK-N-BE2 cells and ENPCs was inhibited by silencing YBX1, but simultaneous treatment with PDYBX1 discounted this inhibition, suggesting that PDYBX1 might act to promote the migration and colonization of ENCCs in the colon. Therefore, PDYBX1 still exerts its protective effect, even when its precursor YBX1 is downregulated in HSCR. Unfortunately, PDYBX1, though upregulated, could not prevent HSCR from progressing into its end stage. This may be because the level of PDYBX1 during the embryonic period is not high enough to completely reverse the impairment of ENS growth. Meanwhile, the downregulation of its precursor protein YBX1 might disrupt the production

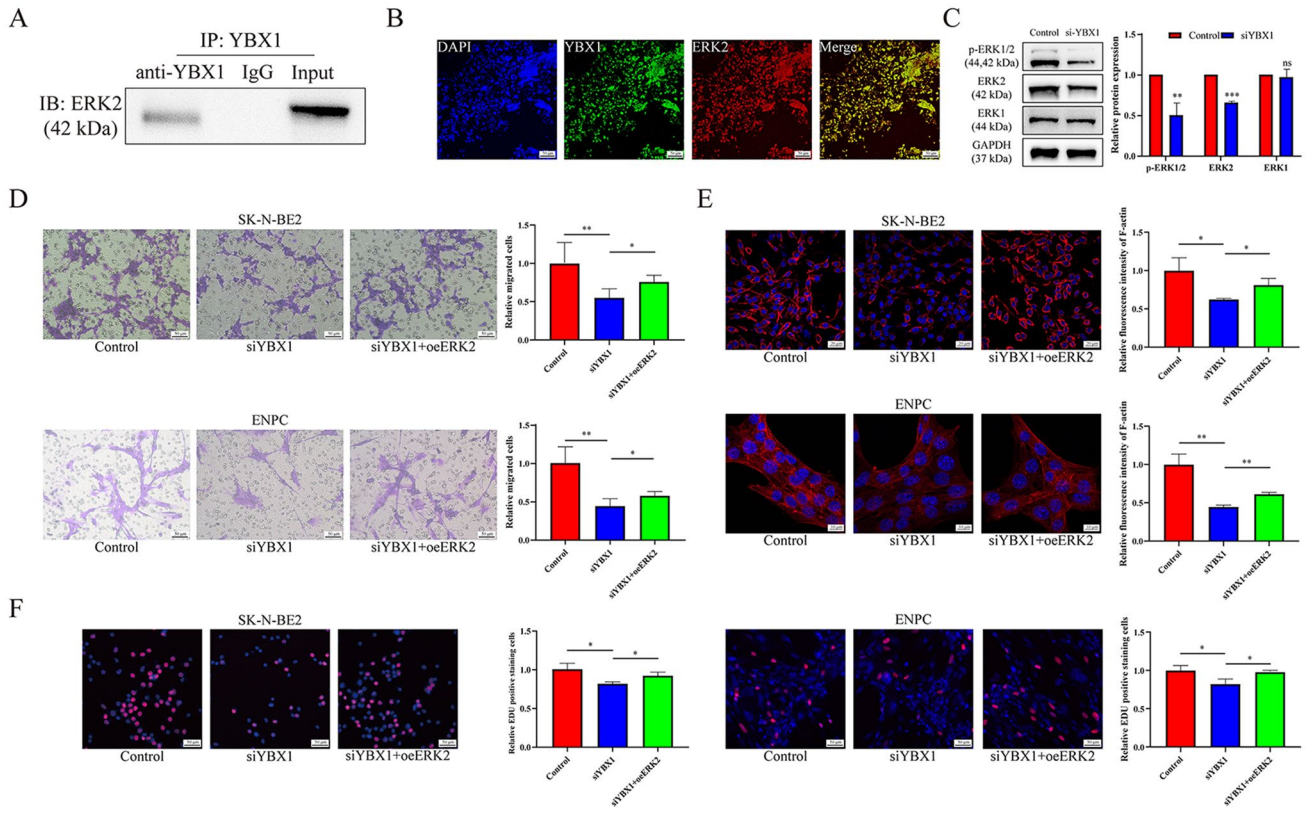

Fig. 5 YBX1 functions by regulating the activation of the ERK1/2 pathway. **A** Co-IP assays show that ERK2 protein is enriched by anti-YBX1 but not anti-IgG in SK-N-BE2 cells. **B** Immunofluorescence showing the colocalization of YBX1 and ERK2 in SK-N-BE2 cells (×20 magnification). **C** Western blots and analysis indicate that silencing YBX1 decreases the expression of both ERK2 and p-ERK1/2, while the expression of ERK1 does not significantly change. **D, E** Transwell assays (×20) and cytoskeleton staining (×63) show that knockdown of YBX1 attenuates cell migration, while overexpression of ERK2 can reverse the inhibitory effect. **F** Overexpression of ERK2 rescues the impaired cell proliferation induced by the downregulation of YBX1 (×20). All cell function experiments were carried out in triplicate. $^{*}P < 0.05$; $^{**}P < 0.01$; $^{***}P < 0.001$.

of PDYBX1, resulting in insufficient output. Besides, apart from the enteric neural cells, other types of cells in the microenvironment of the colon may also take up PDYBX1, leading to the "waste" of PDYBX1. To elucidate the potential therapeutic value of PDYBX1 for HSCR, we established the mouse Ednrb$^{-/-}$ model of HSCR. It is noteworthy that the intervention of PDYBX1 partly reversed the diminishing of enteric neural cell migration in the aganglionic colon of Ednrb$^{-/-}$ mice, indicating that PDYBX1 might promote the formation of the ENS. PDYBX1 injection did not induce the complete colonization of the entire colon by enteric neural cells, which may be explained by the fact that HSCR is a complex congenital malformation caused by multiple factors. Nevertheless, supplementation of exogenous PDYBX1 might be a promising adjuvant therapeutic strategy for HSCR. Furthermore, to determine the efficacy of PDYBX1 in patients with HSCR, more clinical trials are required.

It is well known that YBX1 functions by binding to other proteins through its carboxyl-terminal ending (aa130-324) [29]. For instance, YBX1 combines with G3BP1 to activate the downstream NF-κB pathway to facilitate the migration of renal carcinoma cells [33]. In addition, a protein-protein interaction network analysis has revealed the bond between YBX1 and ERK2 [19]. In prostate cancer, YBX1 specifically binds to ERK2. The expression of ERK2, as well as the phosphorylation of ERK1/2, is repressed as YBX1 is silenced [28]. The ERK1/2 signaling pathway is involved in embryonic development, especially ERK2. An *in vivo* experiment has shown that mice with ERK2 knockout die at 6.5 embryonic days of age, while those with ERK1 knockout survive and present no obvious phenotypes, suggesting that ERK2 may override ERK1 in regulating embryonic development [34, 35]. More importantly, ERK2 is strongly engaged in the development of neural crest cells, indicating its critical role in the activities of the nervous system [36]. Thus, whether YBX1 functions by binding to ERK2 to influence the construction of the ENS during the progression of HSCR needs to be revealed. In this study, we verified the interaction between YBX1 and ERK2 by using immune coprecipitation and immunofluorescence assays. Meanwhile, our findings

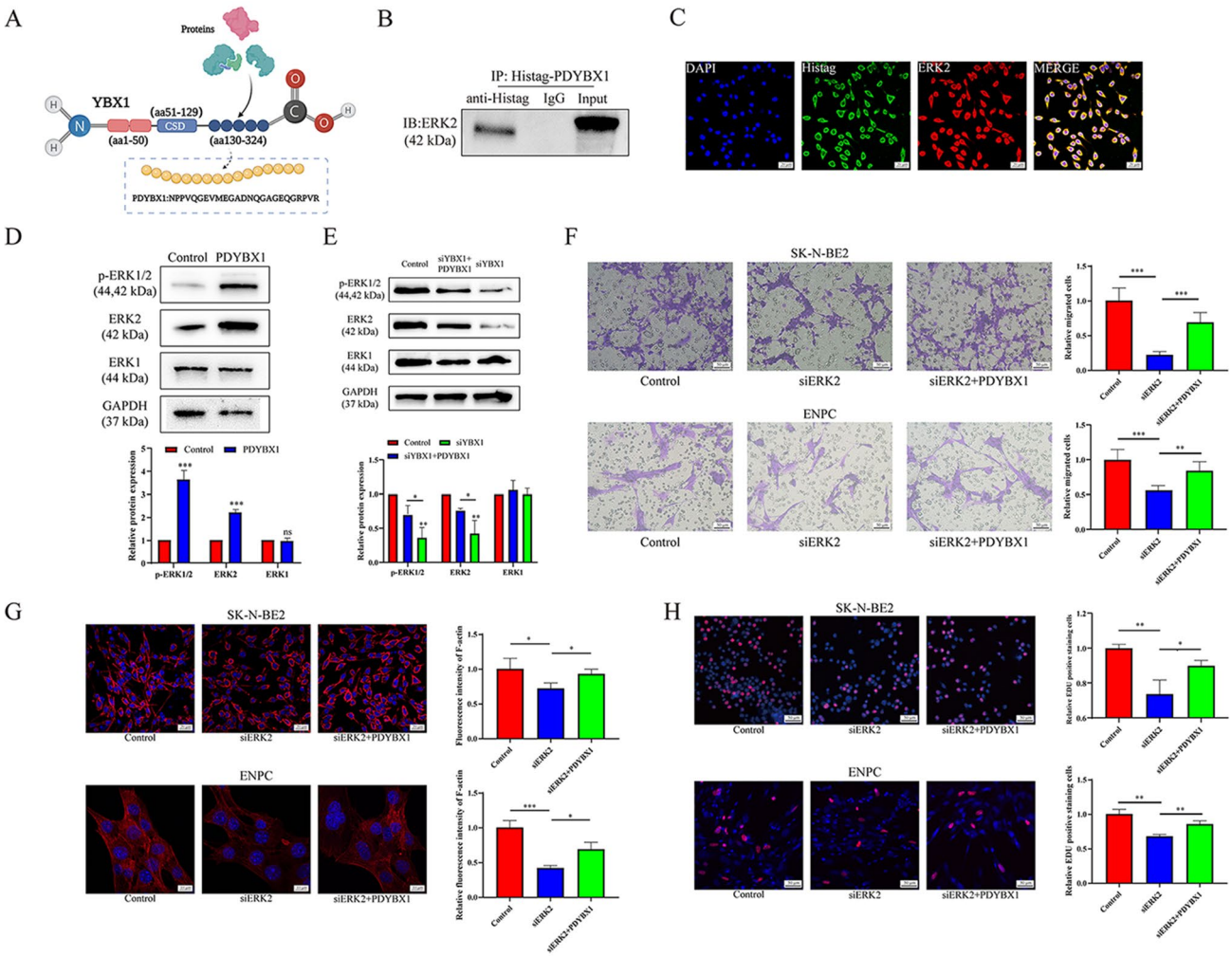

Fig. 6 PDYBX1 promotes cell migration by activating the ERK1/2 pathway. **A** Smart analysis shows that PDYBX1 is located in the carboxyl-terminal (aa 130-324) of YBX1. **B** Co-IP assays show that ERK2 is enriched by anti-Histag but not anti-IgG in SK-N-BE2 cells. **C** Immunofluorescence shows the colocalization of Histag-PDYBX1 and ERK2 (×63). **D** Western blots and analysis indicate that adding PDYBX1 can upregulate the expression of both ERK2 and p-ERK1/2, while the expression of ERK1 is not markedly changed. **E** Treatment with PDYBX1 elevates the protein levels of ERK2 and p-ERK1/2, which are reduced by the downregulation of YBX1. **F, G** Down-regulated ERK2 inhibits the migration (×20) and cytoskeleton formation (×63) of SK-N-BE2 cells and ENPCs, while supplementation with PDYBX1 can alleviate the inhibition. **H** By adding PDYBX1, the impaired cell proliferation caused by the knockdown of ERK2 is rescued (×20). All cell function experiments were carried out in triplicate. $^{*}P<0.05$; $^{**}P<0.01$; $^{***}P<0.001$.

elucidated that knockdown of YBX1 decreased the expression of ERK2, then inhibited the activation of p-ERK1/2, and subsequently impeded the migration of enteric neural cells. Nevertheless, whether YBX1 can affect the colonization of enteric neural cells *via* other signaling pathways needs further study.

Meanwhile, the binding between PDYBX1 and ERK2 was also confirmed. Given that the amino-acids of PDYBX1 are specifically located in the carboxyl-terminal (aa130-324) of YBX1, PDYBX1, and YBX1 may also competitively bind to ERK2 to influence cellular processes involved in HSCR. While the silence of YBX1 arrested the activation of the ERK1/2 pathway, the treatment with PDYBX1, however, enhanced the expression of ERK2, as well as the phosphorylation of ERK1/2. Therefore, PDYBX1 might compensate for the negative effects on the migration of enteric neural cells by reactivating the ERK1/2 signaling pathway which had been inhibited by the downregulation of YBX1. Although ERK2 has been shown to be the common target for YBX1 and PDYB1 in the present study, both may also competitively bind to other proteins that are related to the development of ENS. More research is urgent in the future.

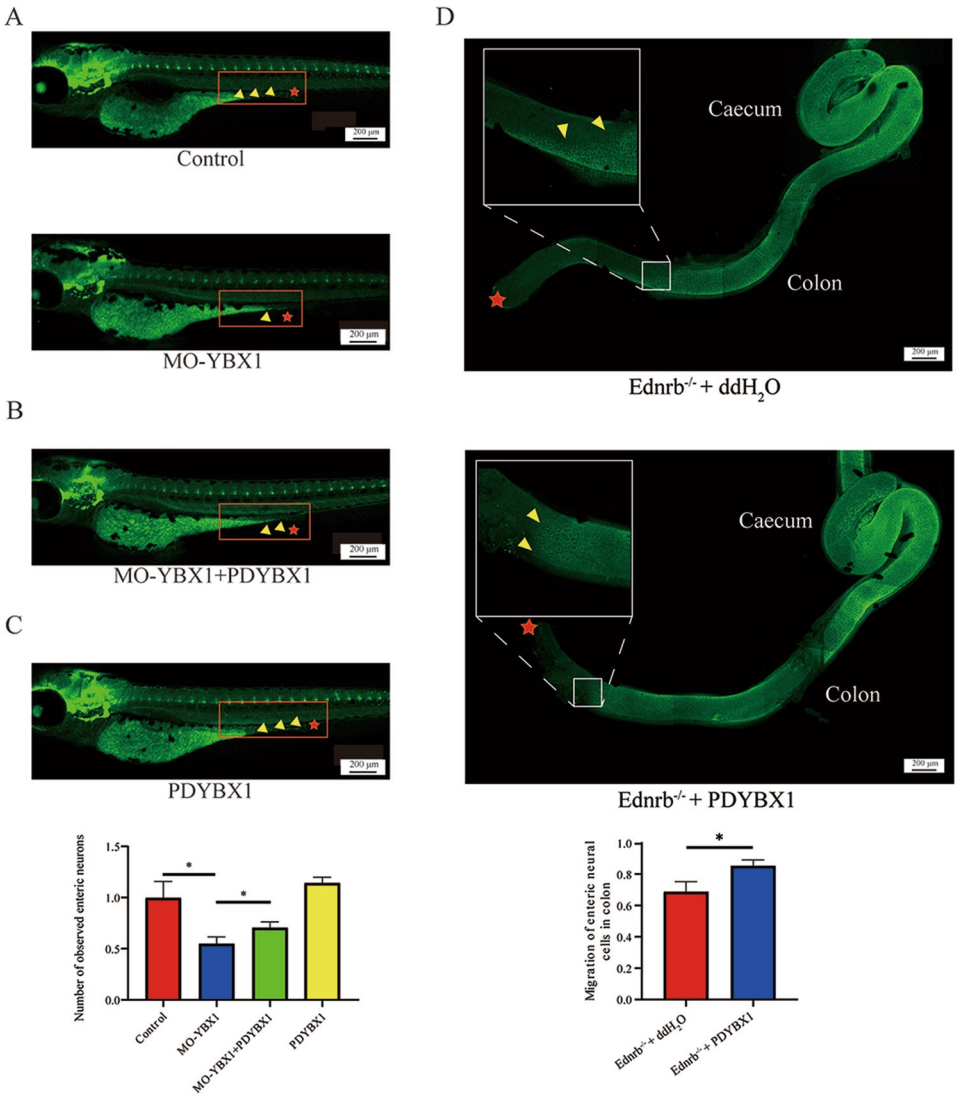

Fig. 7 PDYBX1 protects the development of the ENS in zebrafish and the Ednrb−/− mouse model. Red stars, location of the zebrafish cloaca; yellow triangles, ganglionic cells; orange box, mid-posterior colon. **A** By using mo-YBX1 to knock down YBX1, zebrafish had fewer HuC/D+ cells than controls at 120 hpf. **B** Simultaneous treatment with PDYBX1 is able to partly raise the number of HuC/D+ cells compared to the mo-YBX1 group. **C** Zebrafish treated with PDYBX1 have more HuC/D+ cells and a farther migration distance than controls but the difference is not statistically significant. (D) PDYBX1 treatment improves the formation of the ENS in the HSCR mouse by promoting the migration of enteric neural cells (yellow triangles, the migration terminal of enteric neural cells; red stars, the end of the intestine), compared to HSCR mice treated with ddH_2O. Each group contained 3 samples. All the images were captured under a laser confocal microscope with ×5 magnification. $*P < 0.05$.

Conclusions

In summary, we found that the expression of YBX1 is downregulated in the aganglionic segment of patients with HSCR, and this downregulation may attenuate the migration of enteric neural cells by repressing the expression of ERK2. However, the endogenous peptide PDYBX1, derived from YBX1, is upregulated to activate the ERK1/2 pathway, thus antagonizing the impairment of the ENS caused by the downregulation of YBX1. Our findings shed new light on the mechanisms of HSCR and the therapeutic potential of PDYBX1. Nevertheless, the mechanism by which PDYBX1 is produced and its precursor protein YBX1 is downregulated in HSCR remains unclear. Other negative feedback mechanisms need to be explored.

Acknowledgements This work was supported by the National Natural Science Foundation of China (82001590, 81801496, and 82270540).

Conflict of interest All authors claim that there are no conflict of interest.

References

1. Lake JI, Heuckeroth RO. Enteric nervous system development: Migration, differentiation, and disease. Am J Physiol Gastrointest Liver Physiol 2013, 305: G1–G24.
2. Bahrami A, Joodi M, Moetamani-Ahmadi M, Maftouh M, Hassanian SM, Ferns GA. Genetic background of Hirschsprung disease: A bridge between basic science and clinical application. J Cell Biochem 2018, 119: 28–33.

3. Jaroy EG, Acosta-Jimenez L, Hotta R, Goldstein AM, Emblem R, Klungland A, *et al*. "Too much guts and not enough brains": (epi) genetic mechanisms and future therapies of Hirschsprung disease - a review. Clin Epigenetics 2019, 11: 135.
4. Ambartsumyan L, Smith C, Kapur RP. Diagnosis of Hirschsprung disease. Pediatr Dev Pathol 2020, 23: 8–22.
5. Hei Ha JL, Hang Lui VC, Hang Tam PK. Embryology and anatomy of Hirschsprung disease. Semin Pediatr Surg 2022, 31: 151227.
6. Gosain A, Frykman PK, Cowles RA, Horton J, Levitt M, Rothstein DH, *et al*. Guidelines for the diagnosis and management of Hirschsprung-associated enterocolitis. Pediatr Surg Int 2017, 33: 517–521.
7. Pan W, Goldstein AM, Hotta R. Opportunities for novel diagnostic and cell-based therapies for Hirschsprung disease. J Pediatr Surg 2022, 57: 61–68.
8. Karim A, Tang CS, Tam PK. The emerging genetic landscape of Hirschsprung disease and its potential clinical applications. Front Pediatr 2021, 9: 638093.
9. Vollesen ALH, Amin FM, Ashina M. Targeted pituitary adenylate cyclase-activating peptide therapies for migraine. Neurotherapeutics 2018, 15: 371–376.
10. Gozes I, Sragovich S, Schirer Y, Idan-Feldman A. D-SAL and NAP: Two peptides sharing a SIP domain. J Mol Neurosci 2016, 59: 220–231.
11. Skorput AGJ, Zhang X, Waataja JJ, Peterson CD, Riedl MS, Kitto KF, *et al*. Involvement of the VGF-derived peptide TLQP-62 in nerve injury-induced hypersensitivity and spinal neuroplasticity. Pain 2018, 159: 1802–1813.
12. Klein R, Mahlberg N, Ohren M, Ladwig A, Neumaier B, Graf R, *et al*. The neural cell adhesion molecule-derived (NCAM)-peptide FG loop (FGL) mobilizes endogenous neural stem cells and promotes endogenous regenerative capacity after stroke. J Neuroimmune Pharmacol 2016, 11: 708–720.
13. Nishida T, Inui M, Nomizu M. Peptide therapies for ocular surface disturbances based on fibronectin-integrin interactions. Prog Retin Eye Res 2015, 47: 38–63.
14. Chowdhury M, Enenkel C. Intracellular dynamics of the ubiquitin-proteasome-system. F1000Res 2015, 4: 367.
15. Wang Y, Su J, Fu D, Wang Y, Chen Y, Chen R, *et al*. The role of YB1 in renal cell carcinoma cell adhesion. Int J Med Sci 2018, 15: 1304–1311.
16. Evdokimova V. Y-box binding protein 1: Looking back to the future. Biochemistry (Mosc) 2022, 87: S5–S145.
17. Martin M, Hua L, Wang B, Wei H, Prabhu L, Hartley AV, *et al*. Novel serine 176 phosphorylation of YBX1 activates NF-κB in colon cancer. J Biol Chem 2017, 292: 3433–3444.
18. Evans MK, Matsui Y, Xu B, Willis C, Loome J, Milburn L, *et al*. Author Correction: Ybx1 fine-tunes PRC2 activities to control embryonic brain development. Nat Commun 2023, 14: 412.
19. Gupta MK, Polisetty RV, Sharma R, Ganesh RA, Gowda H, Purohit AK, *et al*. Altered transcriptional regulatory proteins in glioblastoma and YBX1 as a potential regulator of tumor invasion. Sci Rep 2019, 9: 10986.
20. Chu PC, Lin PC, Wu HY, Lin KT, Wu C, Bekaii-Saab T, *et al*. Mutant KRAS promotes liver metastasis of colorectal cancer, in part, by upregulating the MEK-Sp1-DNMT1-miR-137-YB-1-IGF-IR signaling pathway. Oncogene 2018, 37: 3440–3455.
21. Zhang E, He X, Zhang C, Su J, Lu X, Si X, *et al*. A novel long noncoding RNA HOXC-AS3 mediates tumorigenesis of gastric cancer by binding to YBX1. Genome Biol 2018, 19: 154.
22. Taylor L, Kerr ID, Coyle B. Y-box binding protein-1: A neglected target in pediatric brain tumors? Mol Cancer Res 2021, 19: 375–387.
23. Livak KJ, Schmittgen TD. Analysis of relative gene expression data using real-time quantitative PCR and the 2 (-Delta Delta C(T)) Method. Methods 2001, 25: 402–408.
24. Yuan Q, Ren Q, Li L, Tan H, Lu M, Tian Y, *et al*. A Klotho-derived peptide protects against kidney fibrosis by targeting TGF-beta signaling. Nat Commun 2022, 13: 438.
25. Li Y, Lv X, Chen H, Zhi Z, Wei Z, Wang B, *et al*. Peptide derived from AHNAK inhibits cell migration and proliferation in Hirschsprung's disease by targeting the ERK1/2 pathway. J Proteome Res 2021, 20: 2308–2318.
26. To K, Fotovati A, Reipas KM, Law JH, Hu K, Wang J, *et al*. Y-box binding protein-1 induces the expression of CD44 and CD49f leading to enhanced self-renewal, mammosphere growth, and drug resistance. Cancer Res 2010, 70: 2840–2851.
27. Chang YW, Mai RT, Fang WH, Lin CC, Chiu CC, Wu Lee YH. YB-1 disrupts mismatch repair complex formation, interferes with MutSα recruitment on mismatch and inhibits mismatch repair through interacting with PCNA. Oncogene 2014, 33: 5065–5077.
28. Imada K, Shiota M, Kohashi K, Kuroiwa K, Song Y, Sugimoto M, *et al*. Mutual regulation between Raf/MEK/ERK signaling and Y-box-binding protein-1 promotes prostate cancer progression. Clin Cancer Res 2013, 19: 4638–4650.
29. Wolffe AP. Structural and functional properties of the evolutionarily ancient Y-box family of nucleic acid binding proteins. Bioessays 1994, 16: 245–251.
30. Luzón-Toro B, Villalba-Benito L, Torroglosa A, Fernández RM, Antiñolo G, Borrego S. What is new about the genetic background of Hirschsprung disease? Clin Genet 2020, 97: 114–124.
31. Feng M, Xie X, Han G, Zhang T, Li Y, Li Y, *et al*. YBX1 is required for maintaining myeloid leukemia cell survival by regulating BCL2 stability in an m6A-dependent manner. Blood 2021, 138: 71–85.
32. Xu J, Ji L, Liang Y, Wan Z, Zheng W, Song X, *et al*. CircRNA-SORE mediates sorafenib resistance in hepatocellular carcinoma by stabilizing YBX1. Signal Transduct Target Ther 2020, 5: 298.
33. Wang Y, Su J, Wang Y, Fu D, Ideozu JE, Geng H, *et al*. The interaction of YBX1 with G3BP1 promotes renal cell carcinoma cell metastasis via YBX1/G3BP1-SPP1- NF-κB signaling axis. J Exp Clin Cancer Res 2019, 38: 386.
34. Frémin C, Saba-El-Leil MK, Lévesque K, Ang SL, Meloche S. Functional redundancy of ERK1 and ERK2 MAP kinases during development. Cell Rep 2015, 12: 913–921.
35. Boulton TG, Nye SH, Robbins DJ, Ip NY, Radziejewska E, Morgenbesser SD, *et al*. ERKs: A family of protein-serine/threonine kinases that are activated and tyrosine phosphorylated in response to insulin and NGF. Cell 1991, 65: 663–675.
36. Newbern J, Zhong J, Wickramasinghe RS, Li X, Wu Y, Samuels I, *et al*. Mouse and human phenotypes indicate a critical conserved role for ERK2 signaling in neural crest development. Proc Natl Acad Sci U S A 2008, 105: 17115–17120.